Experimental and numerical studies of hydrogen enrichment impact on a non-adiabatic confined swirled flame.

R. Mercier*[1,2], T. F. Guiberti[1,2], L. Zimmer[1,2], D. Durox[1,2], O. Gicquel[1,2], N. Darabiha[1,2], T. Schuller[1,2] and B. Fiorina[1,2]

[1] CNRS, UPR 288, Laboratoire d'Energétique Moléculaire et Macroscopique, Combustion (EM2C), Grande voie des vignes, 92290 Châtenay-Malabry, France.

[2] Ecole Centrale Paris, Grande voie des vignes, 92290 Châtenay-Malabry, France.

Abstract

This work focuses on the experimental and numerical investigations of the shape taken by confined turbulent flames stabilized over a bluff-body swirl injector. Two configurations, which correspond to two levels of H_2 enrichment in the fuel, are investigated. Experiments show that high H_2 concentrations promotes M-shaped flames, whereas V-shaped flames are observed for low values of H_2 enrichment. For both cases, cold and reactive flow LES calculations were performed. Assuming a fully adiabatic combustion chamber, LES always predicts an M-shaped flame and does not capture the V to M shape transition observed in the experiment when the hydrogen concentration is increased. By accounting for non-adiabaticity, simulations predict the correct flame stabilization for both V and M-shaped flames and show good agreement with experiments.

1 Introduction

The shape taken by the flame in a combustor is an important feature that affects the temperature field and pollutant emissions. For a sufficiently large swirl [1], the typical flow structure in a confined swirled combustor is illustrated in Fig. 1. It features two recirculation zones, the inner recirculation zone (IRZ) and the outer recirculation zone (ORZ), which are both composed of burnt gases. Fresh and burnt gases are separated by an inner and an outer shear layers, named ISL and OSL, respectively. The flames generally have a V shape if the combustion reaction only takes place at the boundaries of the ISL of the swirling jet of reactants in contact with the IRZ of burnt products (Fig. 1a-b). If combustion also takes place between the outer shear layer (OSL) of the jet and the external recirculation zone (ORZ) of burnt gases, the flame stabilizes with an M shape (Fig. 1c).

Experimental analysis of these transitions has been recently carried out at EM2C laboratory on a non-adiabatic confined swirled flame [2]. It shows that the topology of swirling flames is highly sensitive to fuel composition and heat transfer to the combustion chamber walls. The numerical prediction of such regimes is therefore very challenging. Indeed, the modeling strategy has to account for numerous physical phenomena such as the combustion chemistry, flame interactions with turbulence, heat losses and fuel composition. Large Eddy Simulation (LES) of turbulent reactive flows is an attractive strategy to capture unsteady phenomena governing combustion dynamics and flame stabilization mechanisms [3]. The recent model F-TACLES (Filtered Tabulated Chemistry for LES) [4, 5], developed to capture the influence of heat losses, turbulence and chemistry on the flame consumption speed, is a good candidate to capture such complex flame stabilization mechanism. As boundary conditions (inlet and walls) were accurately characterized in the EM2C combustor [2], the resulting experimental database is a useful benchmark target for turbulent combustion model validation.

The present article is organized as follow. The swirled combustor configuration is first presented. The experimental diagnostics, the numerical strategies along with the investigated operated conditions are secondly described. Analysis is then carried out to examine the ability of F-TACLES to capture both V and M flame stabilization processes.

*Corresponding author: benoit.fiorina@ecp.fr

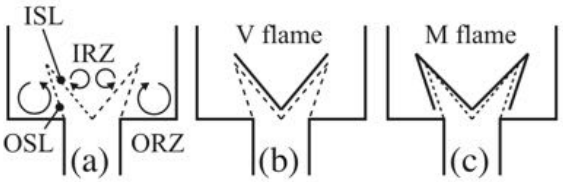

Figure 1: (a) Schematic of a swirling jet flow in a combustion chamber with its inner (ISL) and outer (OSL) shear layers and the inner (IRZ) and outer (ORZ) recirculation zones. (b) V flame. (c) M flame.

2 Swirled confined combustor

2.1 Experimental setup and diagnostics

The experimental setup presented in Fig. 2 features an axisymmetric burner fed by premixed methane, hydrogen and air, includes a cylindrical injection tube with an exit diameter of 14 mm. The flow is put in rotation by a radial swirling vane located upstream of the injection tube. A central rod of 6 mm diameter crossing the swirler is installed on the burner axis to help flame stabilization at the injection tube outlet located 2 mm above the injection plane. To ensure a nearly uniform velocity profile at the entrance of the swirler, the mixture enters the burner through a plenum and subsequently passes through a set of grid/honeycomb/grid arrangement before entering a water-cooled convergent nozzle. The flame is confined by a transparent square chamber featuring four 250 mm (height) $\times$ 92 mm (width) $\times$ 12 mm (thickness) quartz windows.

Mean and Root Mean Square (RMS) axial (U_z) and radial (U_x) velocity profiles are measured with Particle Imaging Velocimetry (PIV). Chemiluminescence imaging of OH* has been carried out to locate the heat release rate. An Abel deconvolution is applied on time-averaged chemiluminescence images to provide the mean reaction zone position in the central longitudinal plane.

The temperature at sold wall of the setup has been determined with two different diagnostics: Laser Induced Phosphorescence (LIP) measurements have been performed to determine the temperature at the quartz walls, at the dump plane and bluff-body wall surfaces of the combustion chamber [2]. Thermocouple measurements were also performed on one of

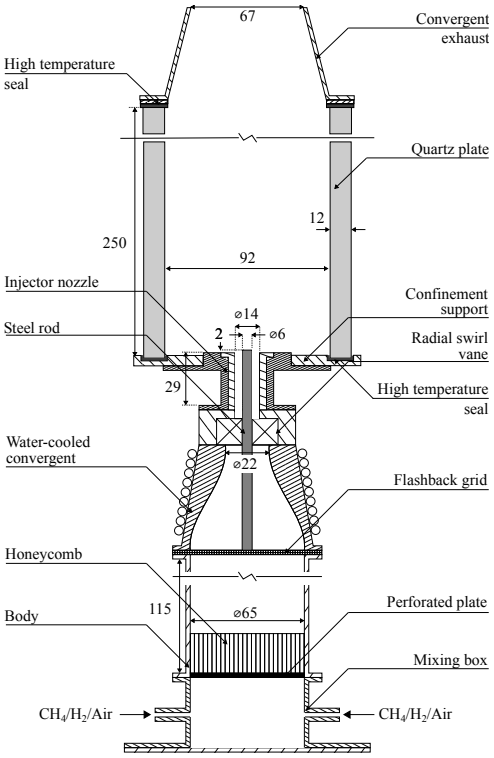

Figure 2: Schematic of the EM2C test rig.

the four vertical steel bars holding the quartz walls at the corners of the combustion chamber. Figure 3 displays the temperature measured on the internal side of one quartz window.

2.2 Numerical setup

Large Eddy Simulation are performed using the YALES2 code [6]. A centered fourth-order finite volume scheme is used for spatial discretization. Time integration of convective terms is performed explicitly using the TRK4 fourth-order scheme [7]. Closure of Reynolds stresses is performed using the SIGMA model [8].

Cold flow simulations have been first performed on a 50 million tetrahedral elements mesh which includes the gas feeding system composed of the swirler and the injection tube. The results of this simulation are used to prescribe the boundary conditions of the reactive flow LES, performed on a shorter domain (composed of 33 million tetrahedral elements), which begin at the bluff-body wall surface axial position.

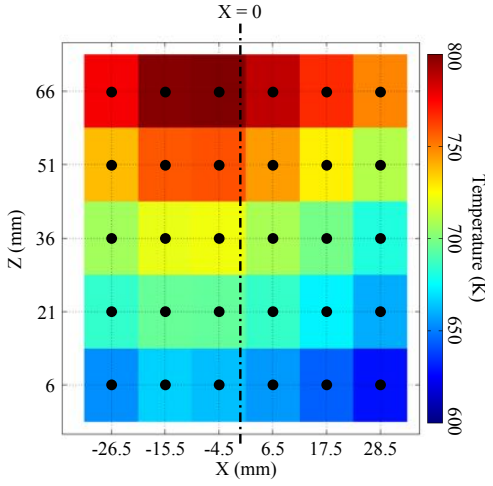

Figure 3: LIP measurements on the quartz window of the combustion chamber.

Numerical simulations are performed with the turbulent combustion model F-TACLES (Filtered Tabulated Chemistry for LES) based on the tabulation of filtered 1-D premixed flames [4]. The impact of heat losses on the chemistry is captured using the formalism developed in [5]. The mean cell size at the flame location goes from 0.25 mm to 0.5 mm, corresponding respectively to 2 and 4 times the laminar flame reaction thickness and 0.5 and 1 times the thermal thickness. The ratio of the filtered flame width versus laminar flame reaction thickness is set to 9 when generating the filtered look-up table. It ensures a sufficient numerical resolution of the filtered reactive layer. The sub-filter scale wrinkling is estimated using the model proposed in [9], with the parameter β set to 0.5. Chemical look-up tables are computed with REGATH thermochemistry package developed at the EM2C laboratory [10, 11] and employing a detailed chemical scheme without accounting for the NOx chemistry leading to 29 species and 141 reactions [12]. The impact of differential diffusion on the flame consumption speed is captured by the tabulation using the methodology developed in [5].

2.3 Operating conditions

A recent experimental study [2] conducted on this test rig showed that flame stabilization process is strongly influenced by heat losses at the combustor wall. In addition, transitions between V and M shapes are observed when increasing the H_2 concentration in CH_4/H_2 fuel blend. Two fuel compositions of $X^{\text{fuel}}_{H_2} = 0.6$ ($X^{\text{fuel}}_{CH_4} = 0.4$) and $X^{\text{fuel}}_{H_2} = 0.9$ ($X^{\text{fuel}}_{CH_4} = 0.1$), which promotes V and M flame shapes, are retained for further analysis. Investigated cases are indicated in Tab. 1. For all cases, the flame power is 4kW and the equivalence ratio is $\phi = 0.7$. The corresponding fresh gases bulk velocity stays around 14 m.s^{-1}. For the $X^{\text{fuel}}_{H_2} = 0.6$ case, both adiabatic and non-adiabatic simulations will be conducted.

Table 1: Simulated cases

Fuel composition	Flame shape	LES	Simu. #
$X^{\text{fuel}}_{H_2} = 0.6$	V	Adiabatic	S1
		Non-adiabatic	S2
$X^{\text{fuel}}_{H_2} = 0.9$	M	Non-adiabatic	S3

3 Results analysis

3.1 Impact of heat losses on flame topology

The influence of heat losses on the turbulent flame structure is investigated through adiabatic (S1) and non-adiabatic (S2) simulations of the configuration with $X^{\text{fuel}}_{H_2} = 0.6$. Figure 4 compares the normalized mean heat release rate predicted by both simulations with the experimental OH* chemiluminescence measurements. Experiments exhibit a V-shaped flame, which is partially explained by local flame extinctions induced

by wall heat losses. Burnt gases flowing inside the outer recirculation zone (ORZ) are cooled by the combustor walls [2]. It leads to local flame extinction and may promote the transition from M to V flame. The adiabatic computation plotted in Fig. 4(b) cannot capture such phenomena and consequently predicts an M-shaped flame where both inner and outer flame fronts are observed. The inner flame front is located in the ISL between the fresh stream and the IRZ filled with burnt products above the bluff-body wall surface. The outer flame front in the OSL delineates the fresh gas stream and the burnt gases in the ORZ. This prediction is not in agreement with the measurements shown in Fig. 4(a), where a V-shaped flame is identified. This contrasts with the non-adiabatic simulation in Fig. 4(c) that captures the flame extinction induced by heat losses. It predicts a V-shaped flame and shows a good agreement with the measurements in terms of flame length and mean opening angle.

The mean and RMS of the radial and axial velocity components are shown in Figs. 6 and 7, respectively. In the present configuration, radial velocity is a very good indicator of thermal expansion due to combustion. The presence of the outer flame front in the adiabatic simulation causes an over prediction of the heat expansion from Z = 5 mm to Z = 20 mm. At the opposite, a better agreement with the experiments is obtained by the non-adiabatic simulation. The difference is also visible on the RMS velocity profiles. It means that the presence of the outer flame front in the OSL damps the flow fluctuations (in the burnt gases) unlike to the non-adiabatic simulation, where heat expansion is reduced. These fluctuations are due to shear layer instabilities developing in the OSL between the injected stream and the slow ORZ. Differences are less visible on the mean and RMS axial velocity profiles shown in Fig. 7 which are both in good agreement with the experiments. The very low and negative mean axial velocities at large radial distances confirms the presence of the ORZ for all axial distances Z where the measurements have been performed.

3.2 Impact of fuel composition on flame topology

Increasing the molar fraction of H_2 in the fuel improves the probability to find a flame front in the OSL [2]. Experiments conducted with $X_{H_2}^{\text{fuel}} = 0.90$ lead to a very high probability to observe a M shape flame. Figure 5 shows the mean flame position for $X_{H_2}^{\text{fuel}} = 0.90$ using mean Abel inverted OH* chemiluminescence measurements. The outer flame front in the OSL, characteristic of an M-shaped flame, is clearly visible. The increase of laminar burning velocity S_l^0 induced by the addition of $X_{H_2}^{\text{fuel}}$ promotes an upstream propagation of the flame front through the OSL [13].

Figure 5 shows the mean flame position predicted by the simulations 3. A good agreement with the experiments is observed. The non-adiabatic extension of the model correctly captures both the effect of heat losses and hydrogen enrichments on the mean flame shape and position.

4 Conclusion

Large Eddy Simulations of a confined swirled combustor have been performed using the turbulent combustion model F-TACLES, based on filtered premixed flamelet tabulation. Two configurations, with two levels of H_2 enrichment in the fuel blend, have been investigated. Experiments show that higher H_2 concentration promotes flames with a M shape, whereas V flames are observed for lower values of hydrogen enrichment. Assuming a fully adiabatic combustion chamber, LES always predicts an M-shaped flame. By accounting for non-adiabaticity, LES predicts the correct flame stabilization and shows good agreement with experiments. In particular, the simulations capture the V to M shape transition when the hydrogen concentration is increased. These comparisons validate the ability of F-TACLES to capture both influences of fuel composition and heat losses on the flame consumption speed, which plays a crucial role in the flame stabilization process.

Acknowledgment

This work was supported by the ANR-10-EESI-05 Grant of the French Ministry of Research and was performed using HPC resources from GENCI-IDRIS (Grant 2013-x20132b0164).

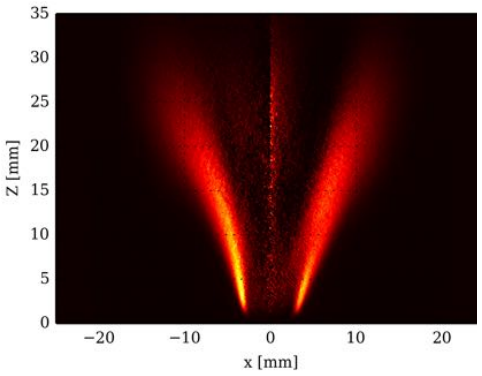

(a) $X_{H_2}^{\text{fuel}} = 0.6$ case. Experiments. Normalized Abel deconvoluted OH* chemiluminescence.

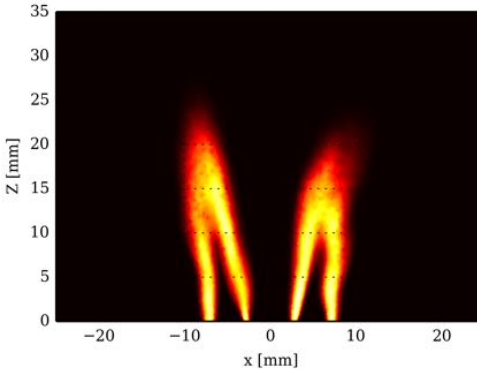

(b) $X_{H_2}^{\text{fuel}} = 0.6$ case. Adiabatic simulation. Normalized mean volumic heat release rate.

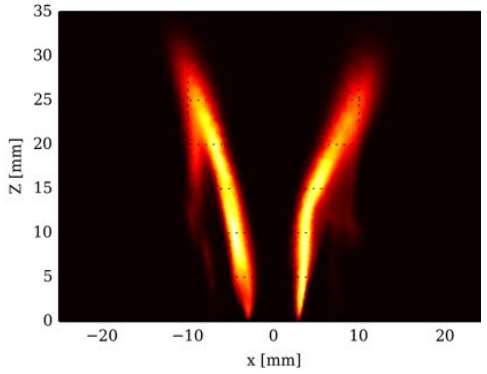

(c) $X_{H_2}^{\text{fuel}} = 0.6$ case. Non-adiabatic simulation. Normalized mean volumic heat release.

Figure 4: Comparisons of the mean flame position between experiments, adiabatic and non-adiabatic simulations.

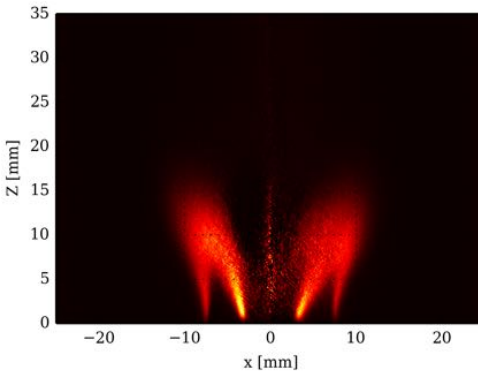

(a) $X_{H_2}^{\text{fuel}} = 0.9$ case. Experiments. Normalized Abel deconvoluted OH* chemiluminescence.

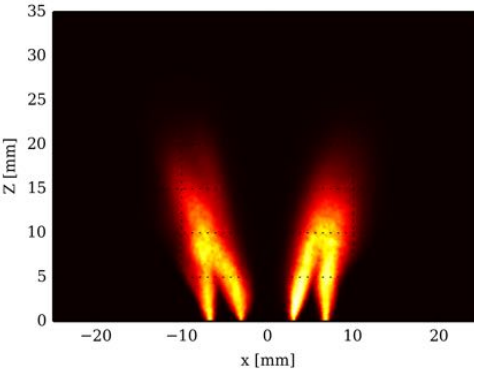

(b) $X_{H_2}^{\text{fuel}} = 0.9$ case. Non-adiabatic simulation. Normalized mean volumic heat release.

Figure 5: Comparisons of the mean flame position between experiments and non-adiabatic simulations.

References

[1] A. K. Gupta, D. G. Lilley, N. Syred, Swirl flows, Tunbridge Wells, Kent, England, Abacus Press, 488p, 1984.

[2] T. Guiberti, D. Durox, P. Scouflaire, T. Schuller, Impact of heat loss and hydrogen enrichment on the shape of confined swirling flames, Proceedings of the Combustion Institute 35 (2) (2015) 1385–1392.

[3] T. Poinsot, D. Veynante, Theoretical and Numerical Combustion, 3rd Edition, 2012.

[4] B. Fiorina, R. Vicquelin, P. Auzillon, N. Darabiha, O. Gicquel, D. Veynante, A filtered tabulated chemistry model for LES of premixed combustion, Combustion and Flame 157 (3) (2010) 465 – 475.

[5] R. Mercier, P. Auzillon, V. Moureau, N. Darabiha, O. Gicquel, D. Veynante, B. Fiorina, LES modeling of the impact of heat losses and differential diffusion on turbulent stratified flame propagation: Application to the TU Darmstadt stratified flame, Flow, Turbulence and Combustion 93 (2) (2014) 349–381.

[6] V. Moureau, P. Domingo, L. Vervisch, Design of a massively parallel CFD code for complex geometries, Comptes Rendus Mécanique 339 (2-3) (2011) 141 – 148.

[7] M. Kraushaar, Application of the compressible and low-Mach number approaches to large eddy simulation of turbulent flows in aero-engines, Ph.D. thesis, Université de Toulouse (2011).

[8] F. Nicoud, H. B. Toda, O. Cabrit, S. Bose, J. Lee, Using singular values to build a subgrid-scale model for large eddy simulations, Physics of Fluids 23 (8) (2011) 085106.

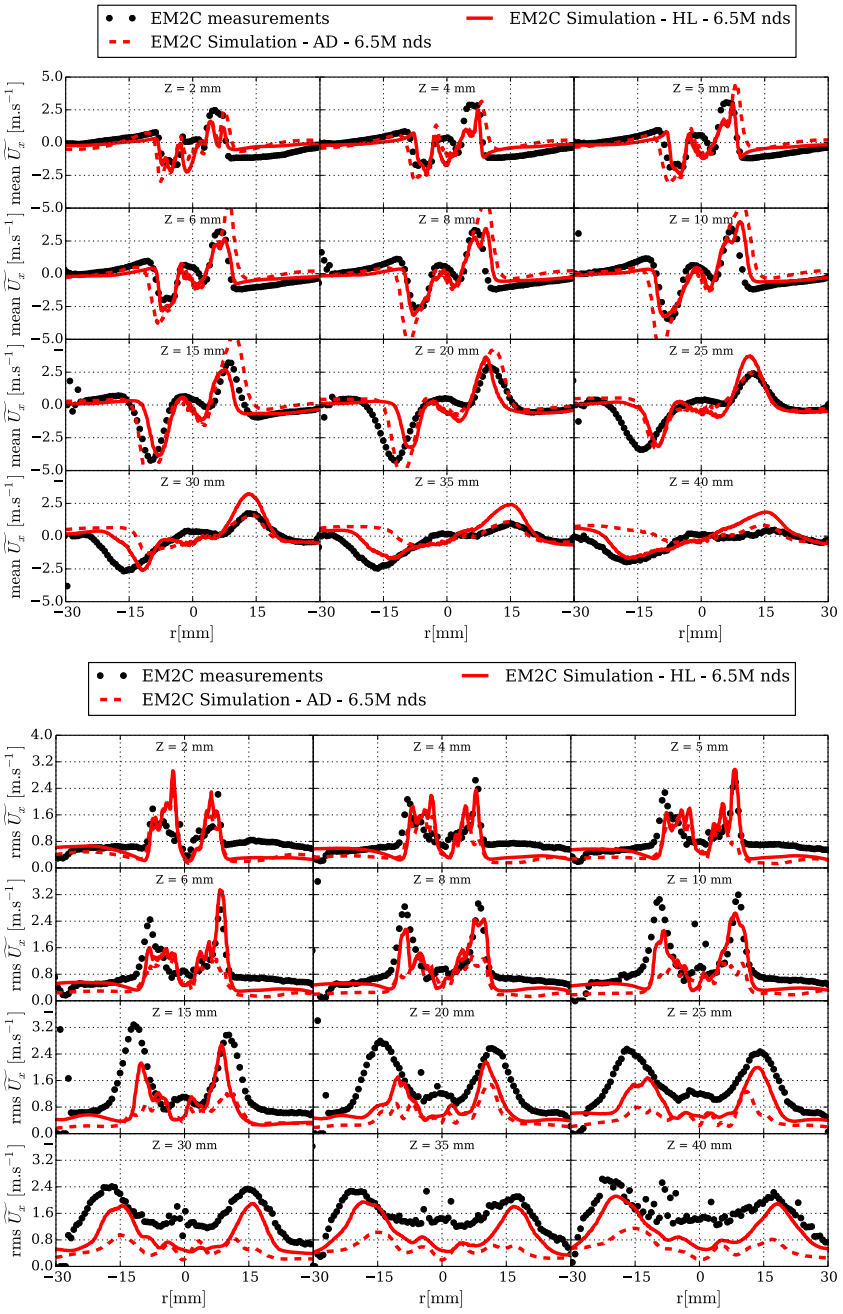

Figure 6: 1-D radial profiles of radial velocity at different distances Z above the bluff-body for the case $X_{H_2}^{\text{fuel}} = 0.6$. Symbols: experiments, dashed lines: adiabatic simulation, solid lines: non-adiabatic simulation. Top: mean profiles. Bottom: RMS profiles.

[9] F. Charlette, C. Meneveau, D. Veynante, A power-law flame wrinkling model for LES of premixed turbulent combustion, part i: non-dynamic formulation, Combustion and Flame 131 (1/2) (2002) 159–180.

[10] L. Pons, N. Darabiha, S. Candel, G. Ribert, V. Yang, Mass transfer and combustion in transcritical non-premixed counterflows, Combustion Theory and Modelling 13 (1) (2009) 57–81.

[11] S. Candel, T. Schmitt, N. Darabiha, Progress in transcritical combustion : experimentation, modeling and simulation, in: 23rd ICDERS, Irvine, 2011.

[12] P. Lindstedt, 12 month progress report 1, Tech. Rep. TR-96 009, Brite Euram Program Project BRPR950056 (1997).

[13] K. T. Kim, J. G. Lee, H. J. Lee, B. D. Quay, D. A. Santavicca, Characterization of forced flame response of swirl-stabilized turbulent lean-premixed flames in a gas turbine combustor, Journal of Engineering for Gas Turbines and Power 132 (4) (2010) 041502–041502.

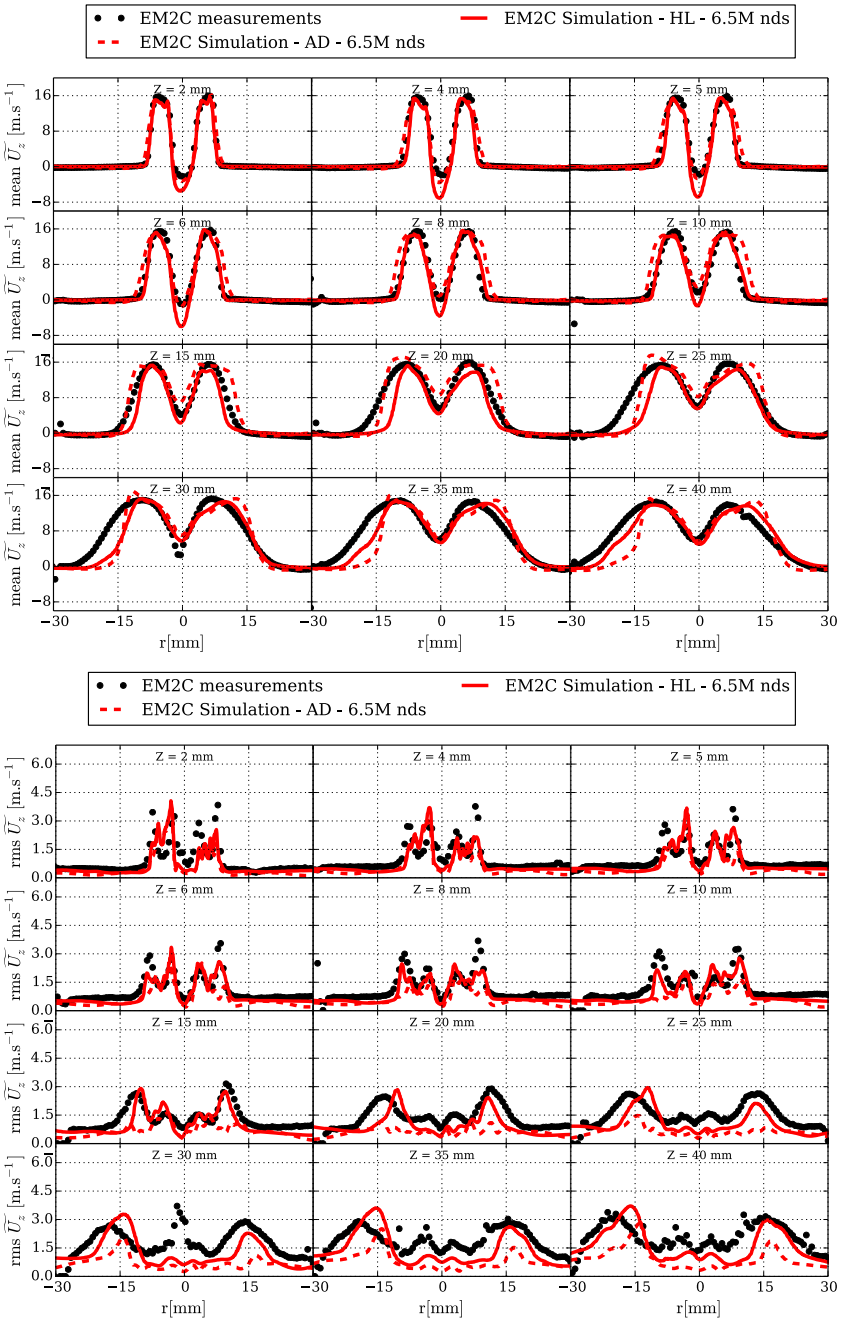

Figure 7: 1-D radial profiles of axial velocity at different distances Z above the bluff-body for the case $X_{H_2}^{\text{fuel}} = 0.6$. Symbols: experiments, dashed lines: adiabatic simulation, solid lines: non-adiabatic simulation. Top: mean profiles. Bottom: RMS profiles.